

Supplementary Information: Novel Pressure-Induced Confined Metal from the Mott Insulator $\text{Sr}_3\text{Ir}_2\text{O}_7$

Yang Ding,^{1,2,3*} Liuxiang Yang,^{1,3} Cheng-Chien Chen,¹ Heung-Sik Kim,⁴ Myung Joon Han,⁴
Wei Luo,⁵ Zhenxing Feng,⁶ Mary Upton,² Diego Casa,² Jungho Kim,² Thomas Gog,² Zhidan Zeng,^{1,3}
Gang Cao,⁷ Ho-kwang Mao,^{1,3,8} and Michel van Veenendaal^{2,9}

¹ Center for High Pressure Science and Technology Advanced Research, Pudong, Shanghai 201203,
China

² Advanced Photon Source, Argonne National Laboratory, Argonne, Illinois 60439, USA

³ HPSynC, Geophysical Laboratory, Carnegie Institution of Washington, Argonne, Illinois 60439,
USA

⁴ Department of Physics, Korea Advanced Institute of Science and Technology, Daejeon 305-701,
Republic of Korea

⁵ Condensed Matter Theory Group, Department of Physics Box 530, SE-751 21 Uppsala, Sweden

⁶ Chemical Sciences and Engineering, Argonne National Laboratory, Argonne, Illinois 60439, USA

⁷ Department of Physics and Astronomy, University of Kentucky, Lexington, Kentucky 40506, USA

⁸ Geophysical Laboratory, Carnegie Institution of Washington, Washington, D. C. 20015, USA

⁹ Department of Physics, Northern Illinois University, De Kalb, Illinois 60115, USA

*yang.ding@hpstar.ac.cn

Jan. 30 2016

A. High-Pressure Resistance Measurements on Single Crystal $\text{Sr}_3\text{Ir}_2\text{O}_7$

The high-pressure electric resistance measurements were performed at room temperature with the standard four-probe-electrode circuit method. A T301 stainless steel gasket was pre-indented to 20 GPa in a symmetric diamond anvil cell, and the thinnest part in the indent was removed. Then, cubic boron nitride/epoxy mixture powders were added inside the indent, which were then pressed to 25 GPa again, reliably insulating the sample and electrodes against the T301 gasket. Si oil is filled as pressure medium for the sample. A hole of $\sim 100 \mu\text{m}$ wide was drilled in the center of cubic boron nitride/epoxy mixture powders and then filled with the sample. A ruby scale was used to determine the pressure. Four gold thin probes ($\sim 2 \mu\text{m}$ thick, labeled respectively as 1, 2, 3, and 4 in Fig. S1) were attached to the samples with sliver glue. By switching the 3 and 2 electrodes, we can get the resistances in the ab -plane and along the c -axis, respectively. The resistances were finally measured up to 63.0 GPa.

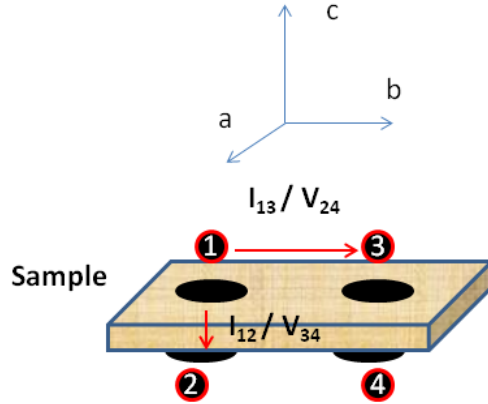


Figure S1. A standard four-probe-electrode circuit setup for high-pressure resistance measurement. The resistances in the ab -plane and along the c -axis can be measured by switching the 3 and 2 electrodes, respectively. The black spots represent the contact points where Au probes are attached to the sample.

B. High-Pressure Resonant Inelastic X-ray Scattering Experiment

$\text{Sr}_3\text{Ir}_2\text{O}_7$ single crystals synthesized using a self-flux technique described in Ref. [1] were used in the high-pressure resonant inelastic x-ray scattering (RIXS) experiment. The single crystal naturally crystallized into a plate-like shape with its c -axis normal to the surface of the plate. In the high-pressure experiment, the single-crystal sample of size $\sim 20 \times 60$ (length and width) $\times 5\text{-}10$ (thickness) μm^3 was loaded with small ruby chips (as pressure markers) into sample chamber surrounded by a beryllium metal or cubic boron nitride gasket, which was then confined in a Mao-type panoramic or symmetric diamond anvil cell. The sample chamber was sealed at ~ 1 GPa with Ne gas as the pressure medium.

The RIXS measurements were performed at beam line 30-ID-B and the newly built 27-ID-B of Advanced Photon Source at Argonne National Laboratory. Incident x-rays were monochromatized by a double-crystal diamond (100) monochromator and a secondary Si(400) channel-cut monochromator. With a spherical diced-bent Si(844) analyzer located two meters away from the sample, the energy resolution of the RIXS spectrometer at Ir L_3 -edge (11216 eV) was determined to be 0.08-0.09 eV (full width at half maximum, FWHM).[2,3] The x-ray beam was focused to the sample position with a spot size $\sim 13 \times 30 \mu\text{m}^2$ (FWHM) at sector 27 ID-B, and $\sim 20 \times 40 \mu\text{m}^2$ at sector 30 ID-B. To suppress elastic scattering signals and maintain the same experimental conditions, the scattering angle 2θ was fixed at 90° in a horizontal scattering plane during all measurements.[4,5]

In the high-pressure RIXS experiments, the loading axis of diamond anvil cell was set to be vertical, in order to allow both incident and scattering x-rays to penetrate the Be or cubic boron nitride gasket window within a horizontal scattering plane. The single crystal was also placed in a specific orientation, so that its c -axis is normal to the scattering plane, while the a - and b -axes are parallel to the incident x-ray beam and detector direction at $2\theta = 90^\circ$, respectively. With such orientation, the reduced scattering vector q is along the $[0, \pi/b, 0]$ direction (assuming a tetragonal symmetry of the sample). From 0.98 GPa to 43.8 GPa, our RIXS data are collected at reduced $q = [0, \pi, 0]$ at 0.98 GPa, $[0, 0.99\pi, 0]$ at 12.4 GPa, $[0, 0.96\pi, 0]$ at 23.6 GPa, $[0, 0.95\pi, 0]$ at 34.4 GPa, and $[0, 0.94\pi, 0]$ at 43.8 GPa, due to the change of lattice parameters at high pressure (Fig. S2 and Table S1). Above 54 GPa, the sample crystal symmetry changes to monoclinic, which is no longer complies with the $[0, \pi/b, 0]$ direction. The lattice parameters are obtained from Ref. [6].

Table S1. The calculation of reduced scattering vector in the 1st Brillouin zone.

Pressure (GPa)	b (Å)	Q (Å ⁻¹)	$g=(1/2,1/2,0)$ (Å ⁻¹)	Q/g	Reduced $Q=[0,k\pi,0]$
0.98	3.8860	8.04	1.14	7.03	1.00
12.4	3.8120	8.04	1.17	6.90	0.99
23.6	3.7330	8.04	1.19	6.75	0.96
34.4	3.6810	8.04	1.21	6.66	0.95
43.8	3.6350	8.04	1.22	6.58	0.94

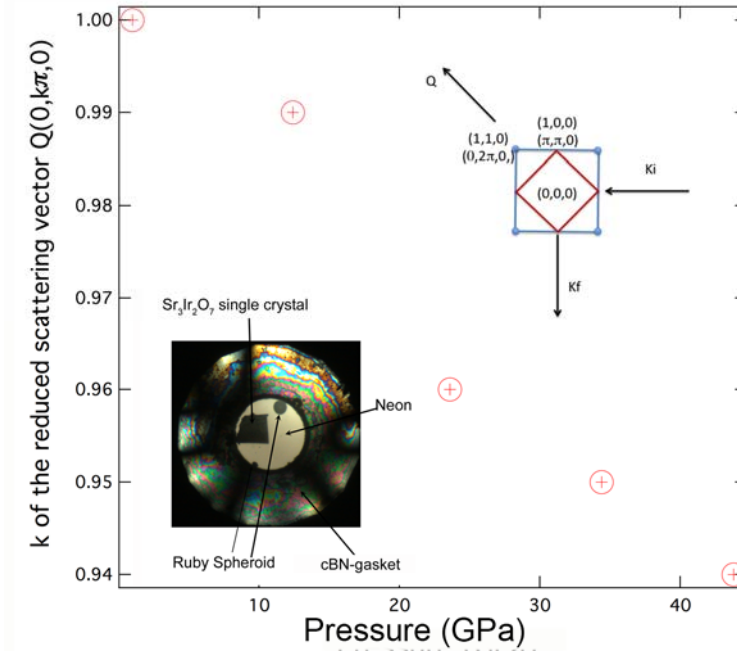


Figure S2. Changes of the reduced scattering vector q due to sample compression at high pressure. The bottom-left inset shows a single crystal $\text{Sr}_3\text{Ir}_2\text{O}_7$ loaded with ruby and Ne in a diamond anvil cell. The culet size is about 400 microns. The top-right inset shows the orientation of the sample.

C. Peak fitting Analysis of Resonant Inelastic X-ray Scattering Measurements

To obtain more accurately the peak positions and line widths, we analyzed the RIXS spectra with the peak-fitting program Igor Pro. The results are plotted in Fig. S3 and S4. To fit peak D, we mainly rely on the RIXS data collected from 0 eV to 6 eV energy loss, while for peak C, we mainly rely on the RIXS data collected from 0 eV to 1 eV energy loss. We note that the line shape of the weak, elastic peak tail is very complicated due to its overlapping with two-magnon and multiple-phonon excitations. To fit such a weak and complicated tail, two Gaussian peaks are most likely not enough. After various trials, we found that at least 3 peaks (two Gaussian-type + one Voigt-type) are required to fit the elastic peak tail, in addition to another Gaussian-type to fit peak C.

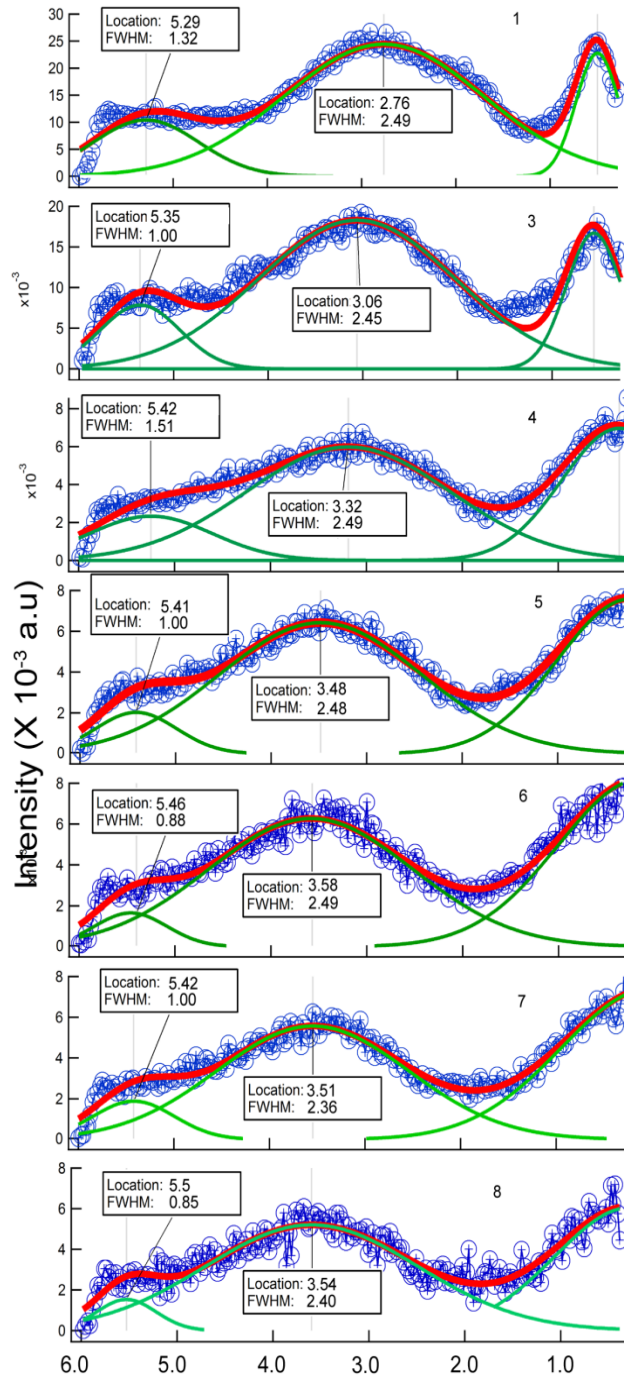


Figure S3. Peak fittings of RIXS data collected in the 0 to 6 eV energy-loss range at various pressures.

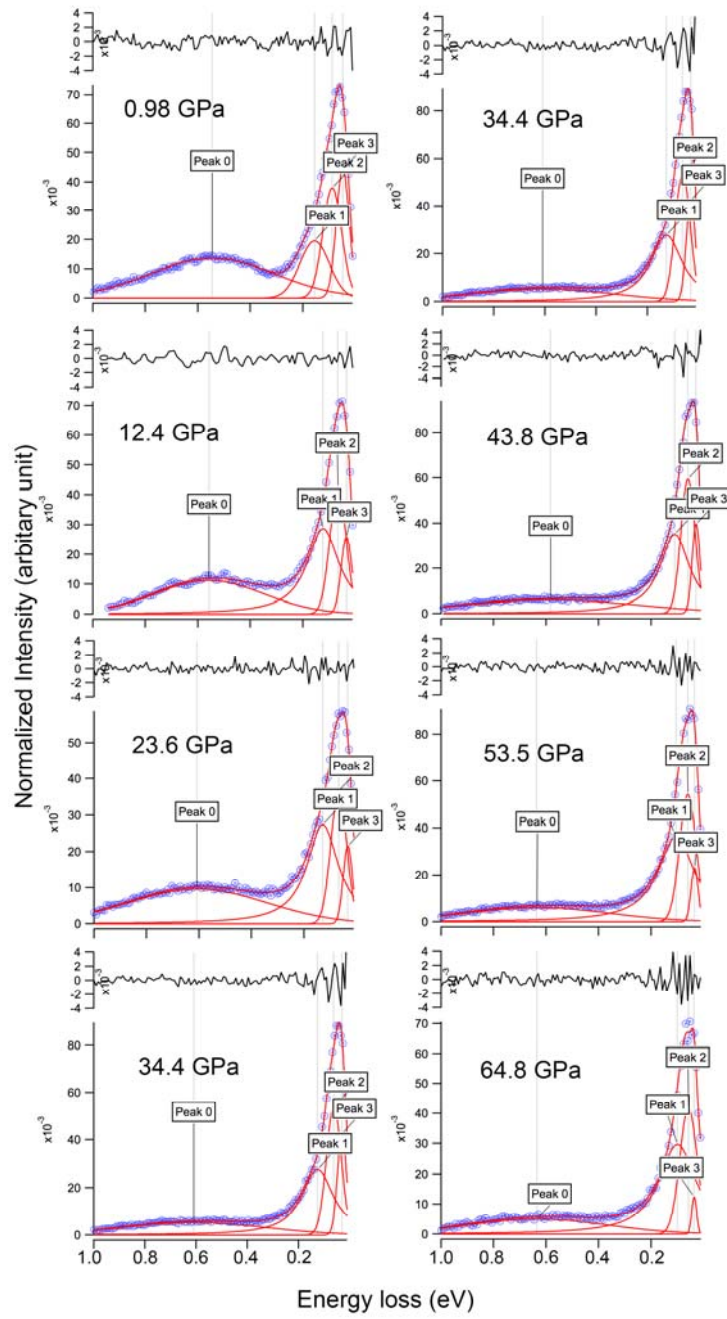


Figure S4. Peak fittings of RIXS data collected in the 0 to 1 eV energy-loss range at various pressures.

D. Calculations of the *ab*-plane Ir-O-Ir bond angle ϕ and Ir-O bond length

The *ab*-plane Ir-O-Ir bond angle ϕ is determined as 158° at ambient conditions, and the orthorhombic lattice parameter a_{orth} is equal to $2^{0.5}$ times the tetragonal lattice parameter a_{tetra} (Fig. S5). In the orthorhombic symmetry, the *ab*-plane Ir-O bond length is $d_{\text{Ir-o}} = \frac{\sqrt{2}}{2} \frac{a_{\text{orth}}}{\sin(\frac{\phi}{2})}$.

By using $\sin\left(\frac{\phi_1}{2}\right) = \frac{d_{\text{Ir-o}}^0}{d_{\text{Ir-o}}^1} * \frac{a_1}{a_0} * \sin\left(\frac{\phi_0}{2}\right) = \left(\frac{10Dq_1}{10Dq_0}\right)^n * \frac{a_1}{a_0} * \sin\left(\frac{\phi_0}{2}\right)$, we could calculate the *ab*-plane Ir-O-Ir bond angle ϕ and Ir-O bond length at high pressure for $n=3.5, 5$ and 7 , respectively.

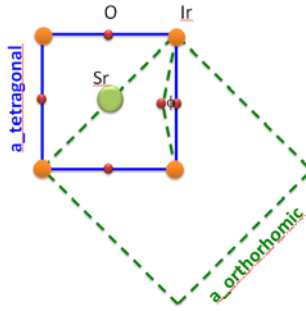


Figure S5. The relationship between the orthorhombic and tetragonal lattices.

The normalized constant K at high pressure, where $K=10Dq*(\text{Ir-O})^n$ ($n=3.5, 5, 7$), is plotted in Fig. S6. By adjusting the values of n , we determined that the normalized K shows the least variation with pressure with $n=4.6$. In another word, when $n=4.6$, the equation $10Dq=K/(\text{Ir-O})^n$ is best complied. This result is comparable to the results in other $5d$ transition-metal oxides. [7]

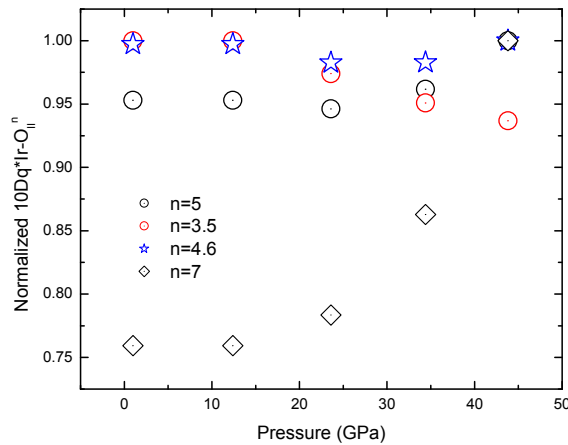


Figure S6. The normalized constant K at various pressures, where $K=10Dq*(\text{Ir-O})^n$.

Table S2. Lattice parameters of Sr₃Ir₂O₇ at high pressure calculated from the equation of state measured by diffraction measurements in Ref. 5.

P	V/V₀	V₀/V	V	a	b	c	B₀	B'
0.00	1.0000	1.0000	318.0000				157.00	4.30
0.98	0.9939	0.9980	316.0538	3.8860		20.9293		
12.40	0.9340	0.9775	297.0120	3.8120		20.4394		
23.60	0.8894	0.9617	282.8133	3.7330		20.2948		
34.40	0.8545	0.9489	271.7246	3.6810		20.0538		
43.80	0.8286	0.9393	263.5012	3.6350		19.9422		
53.50	0.8053	0.9304	256.0759	3.8520	3.5410	18.7740		
64.80	0.7814	0.9210	248.4693	3.8300	3.5120	18.4722		

- [1] G. Cao, Y. Xin, C. Alexander, J. Crow, P. Schlottmann, M. Crawford, R. Harlow, and W. Marshall, *Physical Review B* **66**, 214412 (2002).
- [2] T. Gog, D. M. Casa, A. H. Said, M. H. Upton, J. Kim, I. Kuzmenko, X. Huang, and R. Khachatryan, *J Synchrotron Radiat* **20**, 74 (2013).
- [3] Y. V. Shvyd'ko *et al.*, *Journal of Electron Spectroscopy and Related Phenomena* **188**, 140 (2013).
- [4] K. Ishii, I. Jarrige, M. Yoshida, K. Ikeuchi, J. Mizuki, K. Ohashi, T. Takayama, J. Matsuno, and H. Takagi, *Physical Review B* **83**, 115121 (2011).
- [5] J. Kim *et al.*, *Physical Review Letters* **108**, 177003 (2012).
- [6] C. Donnerer *et al.*, arXiv:1508.04320v1 (2015).
- [7] M. G. Brik, *Journal of Physics and Chemistry of Solids* **68**, 1341 (2007).